

Luminescent properties of $\text{YBO}_3\text{:Eu}^{3+}$ nanosheets and microstructural materials consisting of nanounits

Guohui Pan^{a,b}, Hongwei Song^{a,*}, Lixin Yu^{a,b}, Zhongxin Liu^{a,b}, Xue Bai^{a,b},
Yangqiang Lei^{a,b}, Libo Fan^{a,b}

^aKey Laboratory of Excited State Physics, Changchun Institute of Optics, Fine Mechanics and Physics, Chinese Academy of Sciences Changchun 130033, PR China

^bGraduate school of Chinese Academy of Sciences, Beijing 100039, PR China

Available online 14 March 2006

Abstract

Pure hexagonal-phased $\text{YBO}_3\text{:Eu}^{3+}$ nanocrystals (NCs) including nanosheets (NSs), bundles of nanobelts (NBs) and quasi-spheres composed of nanotubes (NTs) were prepared by hydrothermal method. The results indicate that in NCs, there exist two symmetry sites of Eu^{3+} ions, the interior (A) and the surface (B), while there exists only one interior site (A) in the bulk. It is important to observe that the electronic transition rate of $^5\text{D}_0\text{--}\Sigma_j ^7\text{F}_j$ of Eu^{3+} at the surface site is improved 3–5 times than that of the interior site.

© 2006 Published by Elsevier B.V.

Keywords: Yttrium orthoborate; Luminescence; Low dimension; Nanomaterials

1. Introduction

Over the last few decades, much interest has been focused on the rare-earth orthoborate LnBO_3 ($\text{Ln} = \text{RE}$), a well-known class of inorganic materials. Studies were undertaken to investigate their structures and optical properties. In particular, pseudo-vaterite-type YBO_3 has received much more attention as candidate for highly efficient phosphors in the plasma display panels (PDPs) and a new generation of Hg-free fluorescence lamps due to their high ultraviolet (UV) transparency and exceptional optical damage threshold [1,2], and also because of their structure uncertainty [3,4]. Since the preparation routes may have significant influence on its structure and spectroscopic properties [5], many methods have been employed to synthesize the YBO_3 materials by flux evaporation process [3], solid-state reaction method [6], sol–gel method [4], sol–gel pyrolysis process [2], etc, obtaining single crystal, or powder materials with micron or nanometer size. Hydrothermal method was also used in the previous works [7–9]; however, the optical properties have not been system-

atically studied. In this work, we prepare with Eu^{3+} -activated YBO_3 different morphologies and sizes of NCs by the same method but under different conditions and characterize their structure and optical properties by time-resolved emission spectra, site-selective excitation spectra and fluorescence dynamics. The results indicate that there exist two symmetry sites of Eu^{3+} ions in NCs, the interior (A) and the surface sites (B), while only one interior site (A) exists in the bulk. It is important to observe that the electric transition rate of $^5\text{D}_0\text{--}\Sigma_j ^7\text{F}_j$ of Eu^{3+} at the surface site is improved 3–5 times of that at the interior site.

2. Experimental details

In a typical synthetic procedure, slightly excess HBO_3 was added into the appropriate amount of $\text{Y}(\text{Eu})(\text{NO}_3)_3$ solution with the doped concentration of 5 mol%, under vigorous stirring. The final pH value of this solution was adjusted to be around 8 by adding dropwise 2 M NaOH solution. After continuous stirring for 1 h, a given volume (80 mL) of milky colloidal solution was transferred into a Teflon bottle (100 mL) held in a stainless steel autoclave and subsequently heated at 160, 180, and 200 °C for 12 h. As the autoclave cooled down to room temperature, the

*Corresponding author. Tel./fax: 86 431 6176320.

E-mail address: hwsong2005@yahoo.com.cn (H. Song).

resultant products were collected, washed with distilled water and alcohol, and dried at 60 °C for 24 h in a vacuum oven. These samples are denoted as a, b and c, in the following description. The bulk powder, labelled as bulk, was also prepared by solid-state reaction method through direct firing of starting materials Y_2O_3 , Eu_2O_3 and HBO_3 at 1100 °C for 6 h in air.

X-ray diffraction patterns (XRD) were obtained on a Rigaku D/max-rA powder diffractometer with Cu-K α ($\lambda = 1.54078 \text{ \AA}$) radiation. TEM images were taken on a JEM-2010 transmission electron micrograph under a working voltage of 200 kV. In the measurement of time-resolved fluorescence spectra, a 266-nm light generated from the fourth-harmonic-generator pumped by the pulsed Nd:YAG laser was used as excitation source. It is with a line width of 1.0 cm^{-1} , pulse duration of 10 ns and repetition frequency of 10 Hz. In the measurement of wavelength-selective experiments, a Rhodamine 6G dye pumped by the YAG:Nd laser was used as excitation source. The spectra were recorded by a Spex-1403 spectrometer, a photomultiplier and a boxcar integrator and processed by a computer.

3. Results and discussion

The XRD patterns indicate that all samples crystallized into the pure hexagonal phase in agreement with the JCPDS card (No. 13-0531). Fig. 1. shows the TEM of all samples. Sample a mainly consists of nanosheets (NSs)

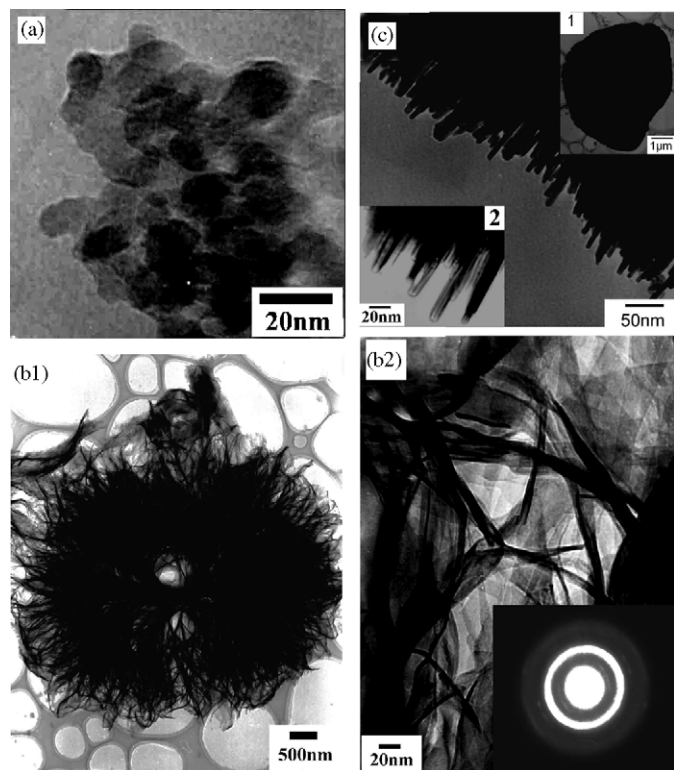


Fig. 1. TEM images of the $\text{YBO}_3:\text{Eu}$ nanocrystals prepared at various hydrothermal temperatures: (a) 160 °C, (b) 180 °C and (c) 200 °C.

with an average length and width of $\sim 10 \text{ nm}$ and thickness of 2–3 nm, while sample b yields micrometer bundles consisting of numerous two-dimensional twisted nanobelts (NBs) (Fig.1(b)). A high magnification TEM image presented in Fig.1(b2) illustrates that a single NB has a width of $\sim 200 \text{ nm}$, thickness of several nanometers and the crinkly surfaces. The selected area electron diffraction (SAED) (inset of Fig.1(b2)) with ring patterns taken from a single NB indicates the formation of polycrystalline YBO_3 . As shown in the inset 1 of Fig.1(c), the sample c yields micrometer quasi-sphere particles. Seen from a section of the surface in Fig.1(c), one particle consists of a great number of nanowires or NTs radiating in all the directions from the center. A highly magnified image (see the inset 2 of Fig. 1(c) illustrates that they are actually NTs with the outer diameter of $\sim 10 \text{ nm}$, growing in all directions from the center.

The photoluminescent properties of $\text{YBO}_3:\text{Eu}^{3+}$ NCs samples were studied and compared with the bulk powders. Fig. 2 shows the time-resolved emission spectra of different NCs and bulk powders. Strong emissions from the $^5\text{D}_0\text{--}^7\text{F}_J$ ($J = 0\text{--}2$) transitions of Eu^{3+} activators were identified in all samples; the red emissions (R) ($^5\text{D}_0\text{--}^7\text{F}_2$) range from 610 to 630 nm, while the orange emissions (O) ($^5\text{D}_0\text{--}^7\text{F}_1$) are located at about 590 nm. Particularly, in sample a, it can be clearly seen that some emissions lines positioned at 588.7, 598.2, 615 and 624.5 nm decay rapidly and almost disappear at 1 ms; while the others still remain, even at 2.5 ms, and the relative proportion of fluorescent emission intensities for $^5\text{D}_0\text{--}^7\text{F}_J$ transitions have less variation, from 1 to 2.5 ms. In contrast, the analogous phenomenon are also observed in the samples b and c. Note that, there are two different features relative to the sample a; first, the content of spectral components corresponding to the rapid decay process decreased due to a weaker intensity; second, a slight blue shift of some emission lines are also observed, typically, the 615 nm emission is blue shifted to about 613 nm. However, we did not observe a rapid decay process other than a constant R/O value (< 1) at a different decay time in bulk. The R/O value is usually used as the measurement of chromaticity of phosphors. In NCs, obviously, the shorter the decay time, the larger the R/O value (> 1). But this value nearly does not change at longer time ($> 1 \text{ ms}$). Thus, the chromaticity is greatly improved in NCs. Here four conclusions can be drawn as: (1) Eu^{3+} activators occupy two crystal symmetry sites in NCs, interior (A) and surface (B) sites, while they occupy only one interior site in bulk. (2) The NCs have improved chromaticity resulting from the luminescence of Eu^{3+} at surface site. (3) The fluorescence lifetime of surface site ($< 1 \text{ ms}$) is much shorter than that of interior site ($> 2.5 \text{ ms}$). (4) The content of Eu^{3+} activators at surface site in sample b and c is lower than that in sample a.

Site selective excitation spectra shown in Fig. 3 perfectly confirm the different symmetry sites distributed in NCs and bulk, and almost the same content of surface site in sample b and c but lower than that in sample a. One reason is that

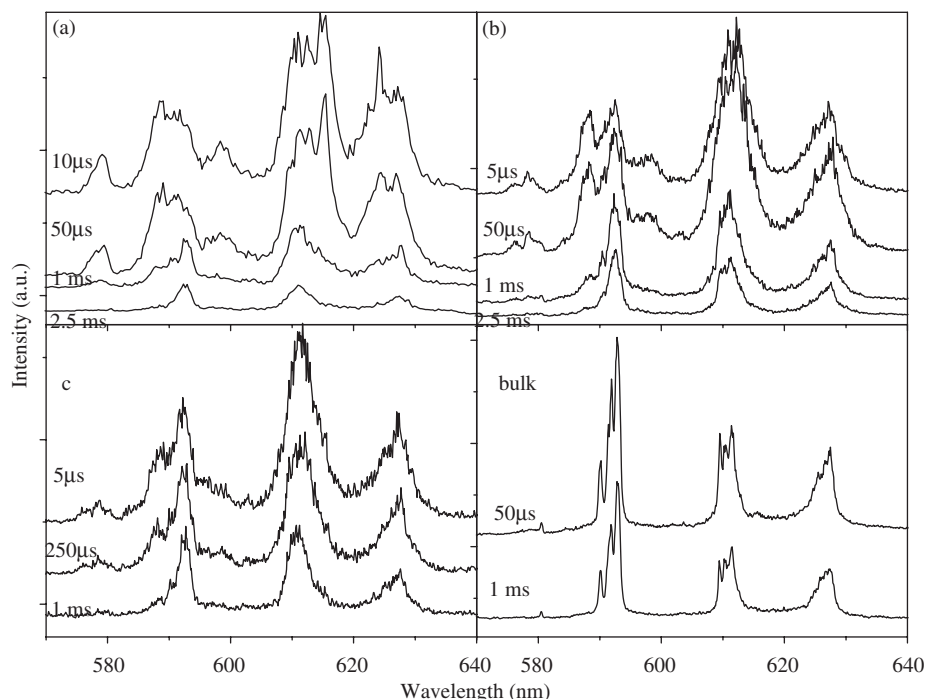


Fig. 2. High-resolution time-resolved emission spectra of Eu^{3+} activators in different NCs and the bulk under 266-nm pulsed laser excitation.

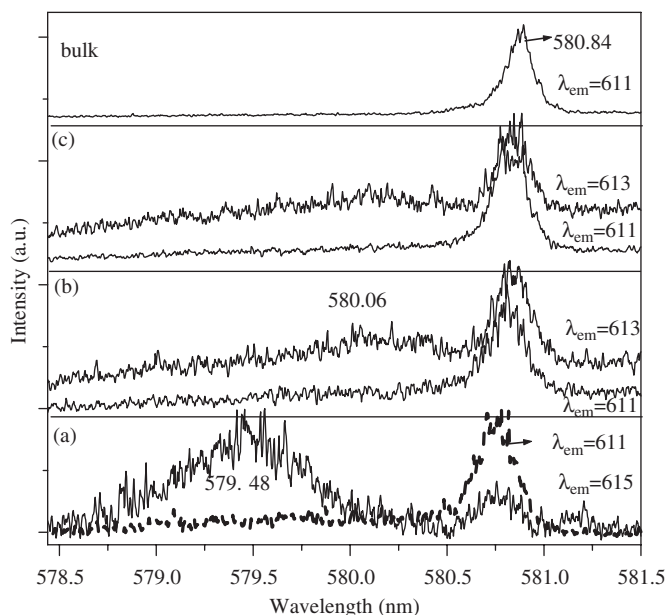


Fig. 3. Site-selective excitation spectra of the ${}^7\text{F}_0$ – ${}^5\text{D}_0$ transitions for Eu^{3+} ions by monitoring different wavelengths.

the larger nanounits for NB and NT in sample b and c than for NS in sample a decrease surface-to-volume ratios in NCs, and the other maybe the close gathering feature in micro-structural materials. The fluorescence lifetime of Eu^{3+} ions at intrinsic and surface site in different NCs and bulk were measured by selective excitation. The fluorescence lifetime at sites (A) and (B) are 2.69 and 0.59 ms in

NSs, 2.35 and 0.93 ms in NBs, 3.66 and 0.95 ms in NTs, respectively, and it is 3.2 ms in the bulk. Coinciding with the above results from the time resolution spectra, the lifetime of Eu^{3+} at surface site is much shorter and decreased to 1/3~1/5 of that of interior site. The electronic transition rates of ${}^5\text{D}_0$ – $\Sigma{}^7\text{F}_J$ for Eu^{3+} activators locating at different symmetry sites in different samples were roughly estimated according to the reverse of fluorescent lifetime [10]. Note that the electronic transition rates of Eu^{3+} activators occupying surface site prominently increase 3–5 times than that of Eu^{3+} activators occupying interior site.

Strictly speaking, the electronic dipole transitions (${}^5\text{D}_0$ – ${}^7\text{F}_2$) are parity forbidden while the magnetic dipole transitions (${}^5\text{D}_0$ – ${}^7\text{F}_1$) are permitted. Thus the former is more sensitive to local environment symmetry than the latter. The nanostructured materials have a larger surface-to-volume ratio, which leads to more activators located at surface or near the surface. The highly disordered surface produce a relatively low local symmetry of site, i.e. the crystal field degeneration, which makes the forbidden-parity of electric dipole transition (${}^5\text{D}_0$ – ${}^7\text{F}_2$) further permitted [10], leading to the increase of electronic dipole transition rate. As a result, the total electronic transition rates of ${}^5\text{D}_0$ – $\Sigma{}^7\text{F}_J$ for Eu^{3+} activators occupying surface site are remarkably increased and generate better chromaticity in NCs.

In conclusion, Eu^{3+} activators in NCs and bulk have different site symmetry distributions; in addition to the interior site existing in bulk, another surface site clearly appears in NCs. Our results also demonstrate that in low-dimensional NCs, the electric transition rate of f–f

inner-shell transitions can be improved largely because of crystal field effect.

Acknowledgement

The authors thank the financial support by National Natural Science Foundation of China (Grants 10374086 and 10504030) and Talent Youth Foundation of JiLin Province (Grants 20040105).

Reference

- [1] D. Boyer, G. Bertrand, R. Mahiou, J. Lumin. 104 (2003) 229.
- [2] Z. Wei, L. Sun, C. Liao, J. Yin, X. Jiang, C. Yan, J. Phys. Chem. B 106 (2002).
- [3] G. Chadeyron, M. El-Ghozzi, R. Mahiou, A. Arbus, J.C. Cousseins, J. Solid State Chem. 128 (1997) 261.
- [4] J.H. Lin, D. Sheptyakov, Y. Wang, P. Allenspach, Chem. Mater. 16 (2004) 2418.
- [5] D. Boyer, G. Bertrand-Chadeyron, R. Mahiou, C. Caperaa, J. Cousseins, J. Mater. Chem. 9 (1999) 211.
- [6] A.M. Srivastava, M.T. Sobieraj, S.K. Ruan, E. Banks, Mater. Res. Bull. 22 (1987) 1455.
- [7] X. Jiang, L. Sun, C. Yan, J. Phys. Chem. B 108 (2004) 3387.
- [8] X. Jiang, C. Yan, L. Sun, Z. Wei, C. Liao, J. Solid State Chem. 175 (2003) 245.
- [9] J. Zhang, J. Lin, J. Cryst. Growth. 271 (2004) 207.
- [10] Q. Tang, J. Shen, W. Zhou, W. Zhang, W. Yu, Y. Qian, J. Mater. Chem. 13 (2003) 3103.